Coiled-coil protein Scy is a key component of a multiprotein assembly controlling polarized growth in *Streptomyces*

Neil A. Holmes[a], John Walshaw[b,c], Richard M. Leggett[a,c], Annabelle Thibessard[a,1], Kate A. Dalton[a,2], Michael D. Gillespie[a], Andrew M. Hemmings[a,d], Bertolt Gust[b,3], and Gabriella H. Kelemen[a,4]

[a]School of Biological Sciences, [c]School of Computing Sciences, and [d]School of Chemistry, University of East Anglia, Norwich Research Park, Norwich NR4 7TJ, United Kingdom; and [b]John Innes Centre, Norwich Research Park, Norwich NR4 7UH, United Kingdom

Edited by Richard Losick, Harvard University, Cambridge, MA, and approved December 7, 2012 (received for review July 5, 2012)

Polarized growth in eukaryotes requires polar multiprotein complexes. Here, we establish that selection and maintenance of cell polarity for growth also requires a dedicated multiprotein assembly in the filamentous bacterium, *Streptomyces coelicolor*. We present evidence for a tip organizing center and confirm two of its main components: Scy (*Streptomyces* cytoskeletal element), a unique bacterial coiled-coil protein with an unusual repeat periodicity, and the known polarity determinant DivIVA. We also establish a link between the tip organizing center and the filament-forming protein FilP. Interestingly, both deletion and overproduction of Scy generated multiple polarity centers, suggesting a mechanism wherein Scy can both promote and limit the number of emerging polarity centers via the organization of the Scy-DivIVA assemblies. We propose that Scy is a molecular "assembler," which, by sequestering DivIVA, promotes the establishment of new polarity centers for de novo tip formation during branching, as well as supporting polarized growth at existing hyphal tips.

bacterial polarized growth | polar multiprotein assembly | cell division | modified hendecad coiled coil

How organisms, cells, or tissues establish polarity is one of the fundamental questions in developmental biology. In eukaryotes, from unicellular organisms to multicellular plants and animals, some of the core mechanisms for generating polarity are conserved (1). Sites for polarization must be selected using positional markers, followed by the recruitment of a complex assembly, which, in turn, orients cytoskeletal filaments that deliver vesicles to the particular sites. A specific example of polarity is polarized growth, during which cells select a single polarization site and generate elongated, cylindrical shapes, such as neuronal dendrites in animals, root hairs and pollen tubes in plants, hyphal growth of filamentous fungi, elongation of *Schizosaccharomyces pombe*, or the short period of polarized growth during budding in *Saccharomyces cerevisiae*. However, the presumed earliest examples of polarized growth can be found in bacteria. These include the actinomycete *Streptomyces coelicolor*, which is used as a model organism for studying morphological differentiation and filamentous growth.

The complex life cycle of *S. coelicolor* begins with an ovoid spore that contains a single chromosome. During germination, long, multigenomic filaments (germ tubes) are formed, which branch regularly to generate a network of hyphal filaments. Branching is a necessity for exponential growth because the rate of tip elongation cannot exceed a certain maximum; hence, there is an exponential increase in the number of new tips. New tips develop on the lateral wall well behind the existing tip, a phenomenon also observed and described as apical dominance in eukaryotic filamentous fungi. When grown on semisolid agar medium, these hyphal filaments first grow across and into the solid medium, generating the vegetative mycelium, followed by the formation of an aerial mycelium by hyphal extension into the air. In addition to branching, the multichromosomal hyphae are segmented by occasional septation, but this is not followed by separation of the neighboring segments. Regular septation is exclusive to the sporogenic aerial hyphae, where a highly coordinated but only partly understood mechanism generates synchronous septation and chromosome segregation, leading to chains of unigenomic spores (2).

The shape of bacterial cells is defined by their cell wall, which largely comprises peptidoglycan. During bacterial growth, peptidoglycan synthesis and deposition does not occur in a random fashion but is highly organized and localized to specific sites identified by cytoskeletal scaffolding proteins. In a typical rod-shaped bacterium, such as *Bacillus subtilis*, there are two phases of nascent peptidoglycan synthesis: during cell division at a midcell division site, where the primary cytoskeletal scaffold is provided by the tubulin-like FtsZ, and during elongation at the lateral wall, where members of the actin-like MreB family, including MreB, Mbl, and MreBH, are implicated in forming the helical pattern of nascent peptidoglycan synthesis (3). In spherical cells such as those of *Staphylococcus aureus*, only the FtsZ-driven cell wall synthesis takes place and occurs at the division site (4), whereas the curved rod-shaped bacterium *Caulobacter crescentus* also employs a third, intermediate filament-like cytoskeletal protein, CreS, to establish its crescent shape (5, 6).

In the filamentous bacterium *S. coelicolor*, hyphal extension takes place exclusively at hyphal tips, as was shown by monitoring fluorescent vancomycin (Van-FL) labeling of newly externalized and/or incorporated peptidoglycan precursors (7, 8). However, the mechanism of polarized growth in *Streptomyces* does not rely on the organization of either MreB helices or FtsZ rings, as is known for common rod-shaped or spherical bacteria. The MreB homologs of *S. coelicolor* are implicated in the development of the rod-shaped compartments that become the spores and not in hyphal tip extension (9–11). Similarly, although *S. coelicolor* FtsZ is essential for septum formation and sporulation, it is not involved in filamentous growth (12). Polarized hyphal extension in *S. coelicolor* depends on the coiled-coil protein DivIVA (8, 13). The *divIVA* gene is essential in *S. coelicolor*, where either partial depletion or overproduction of DivIVA resulted in aberrant

Author contributions: N.A.H. and G.H.K. designed research; N.A.H., J.W., R.M.L., A.T., K.A.D., M.D.G., B.G., and G.H.K. performed research; J.W., R.M.L., and A.M.H. analyzed data; and J.W., A.M.H., and G.H.K. wrote the paper.

The authors declare no conflict of interest.

This article is a PNAS Direct Submission.

[1]Present address: Université de Lorraine, Genetique et Microbiologie, Unité Mixte de Recherche, Institut National de la Recherche Agronomique, BP239-54506 Nancy, France.

[2]Present address: ImmBio, Babraham Research Campus, Cambridge CB22 3AT, United Kingdom.

[3]Present address: Eberhard-Karls-Universität Tübingen, 72074 Tubingen, Germany.

[4]To whom correspondence should be addressed. E-mail: g.kelemen@uea.ac.uk.

See Author Summary on page 1580 (volume 110, number 5).

This article contains supporting information online at www.pnas.org/lookup/suppl/doi:10.1073/pnas.1210657110/-/DCSupplemental.

branching and altered hyphal characteristics (8, 14). DivIVA-Egfp localized to growing hyphal tips and also to sites in the lateral wall, marking future branch points before the appearance of the new lateral tip (14). This suggested that DivIVA was a positional marker for site selection of de novo lateral branch formation. Interestingly, in the rod-shaped actinomycetes *Corynebacterium glutamicum*, *Mycobacterium smegmatis*, and *Mycobacterium tuberculosis*, nascent peptidoglycan synthesis also appears to be directed at the poles in a DivIVA-dependent manner (15), a pattern apparently specific to actinomycetes. The direct interaction between DivIVA and PBP3, a penicillin-binding protein in *M. tuberculosis* (16), supports the role of DivIVA as a polarity marker that recruits the cell wall synthetic machinery during polarized growth in actinomycetes.

DivIVA itself is widespread in Gram-positive bacteria but has different roles outside of the actinomycetes. In *B. subtilis*, for example, DivIVA controls cell division via positioning of the MinC and MinD division inhibitor proteins to the cell poles, allowing FtsZ ring formation at midcell (17). In *B. subtilis*, DivIVA localizes to the midcell during cell division and to mature cell poles by targeting to negatively curved, concave membranes (18, 19).

Apart from the site selection for cell wall extension by DivIVA in the actinomycetes, such as *S. coelicolor*, *C. glutamicum*, *M. smegmatis*, and *M. tuberculosis*, very little is known of the mechanism and the molecular interactions that drive polarized growth in bacteria. Here, we report that although DivIVA is necessary, it is not sufficient for normal polarized growth in *Streptomyces*, and we present Scy (*Streptomyces* cytoskeletal element), a unique coiled-coil protein, which, together with DivIVA, is critical for establishing and maintaining polarized growth in *S. coelicolor*. We provide evidence of a complex, multiprotein, polar assembly for polarized growth in bacteria, and we demonstrate that Scy controls the number of new polarity centers established.

Results

Scy Is a Large Coiled-Coil Protein with a Unique Periodicity. Homologs of actin-, tubulin-, and filament-forming proteins have been identified in *Streptomyces* [MreB (9); FtsZ (12), and FilP (20), respectively]. Our search to find additional bacterial homologs of eukaryote cytoskeletal proteins revealed a large protein of 1,326 amino acid residues (M_r = 146 kDa) encoded by *SCO5397* of *S. coelicolor*. This gene product has a net negative charge and an estimated pI of 4.94 with a highly skewed amino acid distribution, being especially rich in Ala, Glu, and Arg. The COILS program (21) predicted a high coiled-coil–forming probability along almost the entire length of the sequence. This, together with the known role of long coiled coils as levers, scaffolds, or spacers of the eukaryote cytoskeleton and supported by the work described below, prompted the designation of Scy. Analysis of the sequence indicated that Scy consisted of three domains (Fig. 1*A*): the N-terminal canonical, coiled-coil domain (residues 1–64) is followed by a short, Gly-rich flexible "hinge" (residues 64–72) and the long C-terminal domain (1,227 residues) composed of a noncanonical, 51-residue repeat (22). Interestingly, the very few (only 4) proline residues flank the N- and C-terminal coiled-coil domains at positions 11, 64, 1,300, and 1,317. The positions of the hydrophobic residues within coiled-coil proteins are crucial for the association of the α-helical strands via hydrophobic interactions. The hydrophobic residues plotted onto the α-helical cylinder suggest a more shallow, right-handed hydrophobic streak in the penindaenad repeat of Scy compared with a steeper, left-handed hydrophobic streak in the canonical heptad repeat (Fig. 1*B*).

BLAST searches identified homologs of Scy exclusively among the filamentous actinomycetes; however, one of the most important features of a long coiled-coil protein, such as Scy, is the periodic occurrence of hydrophobic residues within the primary sequence, for which BLAST and other sequence similarity search approaches are far less suitable than fast Fourier transforms (FTs). The very sharp and strong FT signal for Scy at 3.643 (Fig. S1) is equivalent to the rational number 51/14, which represents a repeat of 51 residues containing 14 approximately equally spaced hydrophobic residues forming the internal interface of the coiled coil. We searched the UniProt database for coiled-coil proteins with repeat periodicity similar to that of Scy, and we found numerous examples of short (<250 aa) coiled coils with putative penindaenad repeats represented in all domains of life. Interestingly, we have also found several proteins with long (~600–1,000 amino acids) Scy-like repeats among bacteria (*Helicobacter*, *Leptospira*, and *Brachyspira)* and simple eukaryotes (*Paramecium* and *Trichomonas*) (Fig. S1).

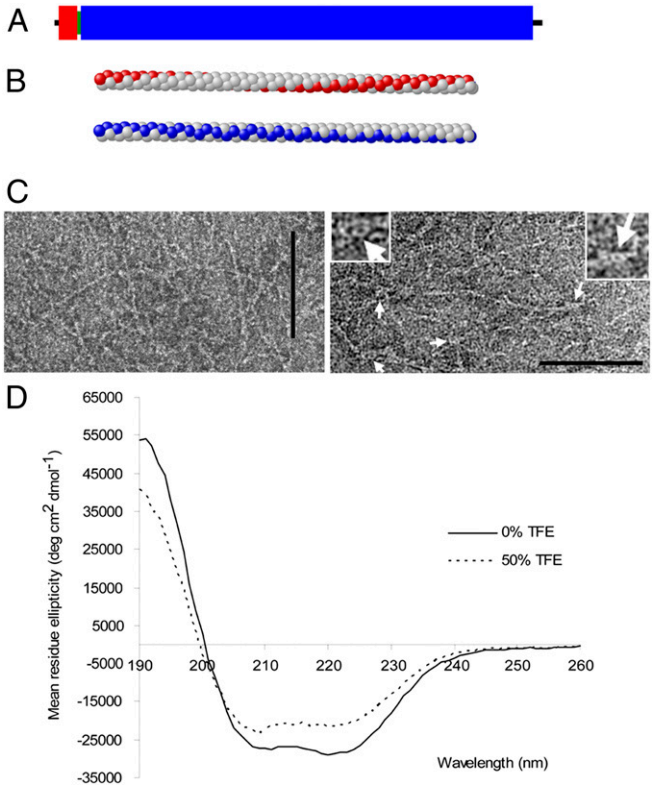

Fig. 1. Scy has a unique coiled-coil structure that forms filaments in vitro. (*A*) Domain structure of Scy from sequence analysis is shown, including the N-terminal canonical (red) and C-terminal 51-residue repeat (blue) coiled coils and the short hinge domain (green) (Fig. S1). (*B*) Atomic model of the α-helix exhibits the stylized left-handed hydrophobic stripe (red) resulting from a canonical heptad repeat. The stylized shallower, right-handed hydrophobic stripe (blue) resulting from the 51-residue repeat, assuming 3.6 residues per turn, is also shown. (*C*) Negative staining of His-Scy using TEM confirmed the filamentous nature of Scy. Occasionally, circular structures (white arrows) could be discerned at the end of the Scy ropes. (*Insets*) Close-up images of these structures are shown. (Scale bars: 100 nm.) (*D*) CD spectroscopy of His-Scy in the absence and presence of 50% (vol/vol) TFE.

Scy Can Form Coiled-Coil Filaments in Vitro. Overexpressed His-tagged Scy, purified from the soluble fraction of *Escherichia coli* cells, formed filaments in vitro, as seen using negative staining and transmission electron microscopy (TEM). We routinely observed a network of rope-like filaments (Fig. 1*C*) that are compatible with our analysis of the coiled-coil sequences of Scy, which predicted a long, flexible rope of ~190 nm for a single Scy coiled coil (22).

CD spectropolarimetry also supported a helical coiled-coil Scy structure (Fig. 1*D*). The far-UV CD spectrum of Scy revealed minima at 208 nm and 222 nm, which is characteristic of a protein with significant α-helical content, and the latter minimum indicated that Scy was 73% α-helical. This degree of α-helicity compares well with that of known coiled-coil proteins at the

same temperature. Another significant feature of Scy's spectrum is a ratio of $[\theta]_{222}/[\theta]_{208} > 1$, indicating a stable coiled coil. Exposure to 50% (vol/vol) trifluoroethanol (TFE), which blocks hydrophobic interactions and so decreases the oligomerization of amphipathic α-helices into coiled coils, changed this ratio in Scy from 1.07 to 0.94. Consistent with its coiled-coil structure, spectral deconvolution of Scy also indicated that the TFE-induced disruption of oligomerization resulted in the decrease of the helical content to 55%, implying cooperativity between helix formation and the coiled-coil assembly.

Deletion of *scy* Affects Polarized Growth and Hyphal Geometry. Null mutants of *scy*, K110 and K111, were generated by replacing *scy* in the *S. coelicolor* chromosome with an apramycin resistance cassette. A further nonmarked *scy* mutant, K112, was created by removing the resistance cassette from K111. The three mutants displayed the same phenotypes, and pK47, carrying *scy*, fully complemented the growth defect of strain K110, suggesting that the *scy* mutation did not have a polar effect on the downstream gene *SCO5396* (*filP*) (20) or that the *scy* mutation was dominant.

Compared with the wild-type (WT) strain, development of the *scy* mutant was severely affected. As a result of the *scy* mutation, individual colony sizes, tested at the same colony density of 100 colonies in a 9-cm–diameter solid medium, were significantly reduced to one-half of the diameter of the WT (Fig. 2*A*). Although K110 did sporulate, it produced ∼10-fold fewer spores than the WT. Further microscopic analyses established that the *scy* mutation had a pleiotropic effect on polarized growth and hyphal characteristics. In WT *S. coelicolor*, new branches formed predominantly at lateral sites and very little apical branching was detectable. Much more abundant branching was observed during hyphal development of K110, with frequent apical branching or tip splitting (Fig. 2 *B* and *C*). This overbranching was characteristic not only of the vegetative hyphae of K110 but of the aerial filaments, which later metamorphosed into branching spore chains. Unlike the uniform chromosome distribution (one chromosome in every prespore) and regular septation of the nonbranched spore chains of WT *S. coelicolor*, both septation and chromosome distribution were highly irregular in the spore chains of K110 (Fig. 2 *D*–*G* and Fig. S2).

Both fluorescence microscopy and TEM confirmed that although the diameter of the WT hyphal cylinder was even

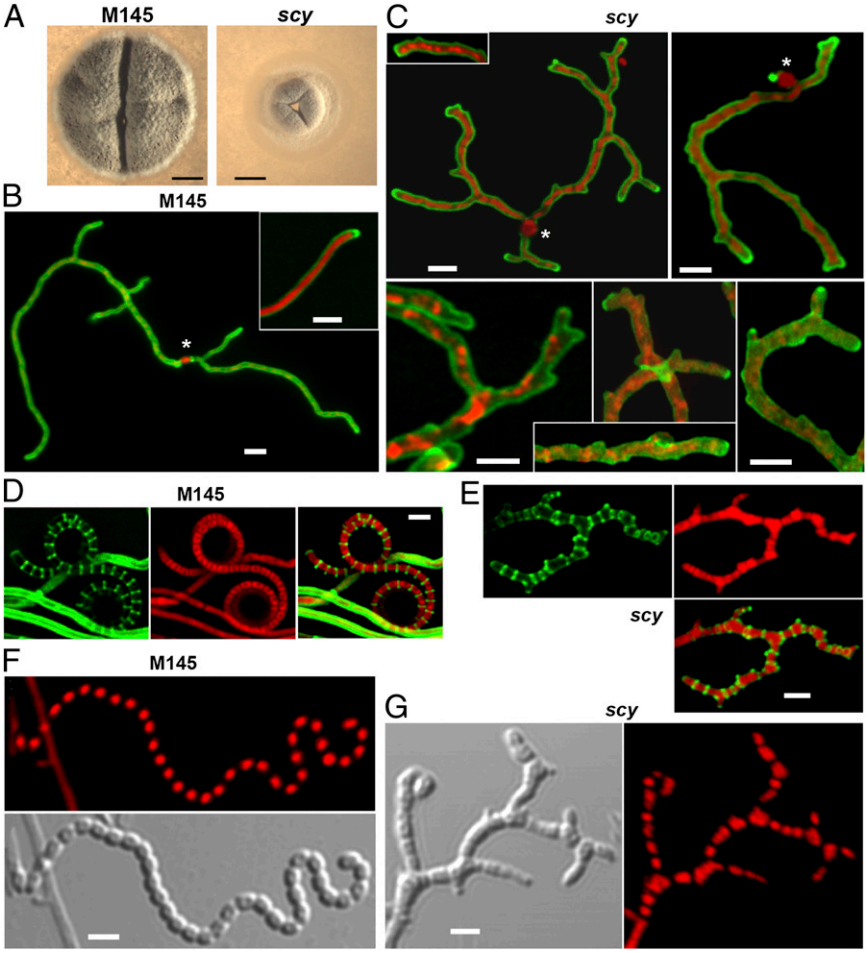

Fig. 2. Mutation of *scy* severely affects polarized growth and development. (*A*) Single colonies of *S. coelicolor* M145 (WT) and K110 (*scy* mutant) are shown after 6 d of growth. To ensure that colony density did not affect growth, we plated a similar number of colonies, ∼100 cfu per plate. (Scale bars: 1 mm.) The WT (*B*) and the *scy* mutant, K110 (*C*), were grown for 16 h, and the branching hyphae originating from single spores (marked with asterisks) were viewed using laser-scanning confocal microscopy after staining the cell wall with WGA-Alexa488 (green) and the chromosomes with propidium iodide (PI; red). Overlaid images of the two fluorescent channels are shown (see also Fig. S2). Early spore chains of the WT (*D*) and the *scy* mutant, K110 (*E*), were stained as above after growth for 44 h alongside microscope coverslips to allow viewing of aerial development and sporulation. Images of the two fluorescent channels are shown separately in addition to the overlaid view. Mature spore chains of the WT (*F*) and the *scy* mutant, K110 (*G*), were stained with PI (red) after growth for 72 h as in *D* and *E*. A differential interference contrast image is also shown. (Scale bars: *B*–*G*, 1 μm.)

throughout its length, varying between 0.4 and 0.7 μm, the *scy* mutant had a very irregular hyphal width, varying between 0.25 and 1.1 μm. Thin cross-sections of the WT hyphal cylinder generated circular or ellipsoidal shapes when the TEM sectioning was nearly perpendicular to the hyphal axis, whereas in the *scy* mutant, irregular "amoeboid" cross-sections were typical (Fig. S2). Because hyphal extension occurs at the hyphal tip in *Streptomyces*, to explain the irregularities in the hyphal diameter of *scy*, we looked for cues in the tip architecture. In the WT, the tip dome was symmetrical with at least one plane of symmetry, whereas the hyphal tip of the *scy* mutant was often bulging and asymmetrical.

Scy Controls Apical Dominance and Cell Wall Synthesis in *Streptomyces*. To characterize the aberrant branching pattern of the *scy* mutant, we analyzed ~300 individual hyphal colonies of both the WT and K110 using microscopy. Each colony originated from a single spore after 10–16 h of incubation on solid medium. The internal segment lengths (i.e., hyphal length between two neighboring branch points) were measured, and a histogram was plotted (Fig. 3*A*). The modes of the segment lengths were 5 μm and 2 μm, whereas the mean values were 7.73 μm and 4.15 μm for the WT and K110, respectively, indicating that multiple branches emerged closer to each other in the *scy* mutant.

Another difference between the WT and the *scy* mutant was related to the phenomenon of apical dominance, namely, the inhibition of lateral branches behind the growing apical tip. We set out to examine the relative positions of new branch points (NB) for emerging new tips (NT) within an existing hyphae (Fig. S3), which itself has an extending tip (T) and originated from a branchpoint (B). As we were analyzing snapshots, we defined new branches as those with lengths <1.5 μm. Histograms of the relative distances of a tip to a new branch point (T to NB) vs. a tip to an old branch point (T to B) were plotted using the same sets of hyphal samples tested above (Fig. 3*A*). Apical dominance was typical for the WT strain, which had a strong preference for generating new tips far behind the growing tip. In the WT, only 6% of the new branch points were in the tip-proximal 20% of the hyphal length, whereas 77% of the new branch points were closer to the previous branch point than to the growing tip. In contrast, in the *scy* mutant, 33% of the new branch points were in the tip-proximal 20% and 66% of new branch points were in the tip-proximal half of the hyphal filament, suggesting the lack of apical dominance in the *scy* mutant.

To test whether the uneven hyphal diameter, the short hyphal length, and the aberrant branching pattern of K110 reflected defects in the incorporation of cell wall precursors, we set out to monitor cell wall synthesis using Van-FL. In unfixed cells, Van-FL cannot pass through the cell membrane but binds to the terminal amino acids of either lipid-linked disaccharide pentapeptide precursors or the as yet non–cross-linked growing cell wall (7). The helical Van-FL staining reflected the helical pattern for peptidoglycan incorporation in the rod-shaped *B. subtilis,* whereas Van-FL localized to the poles/tips of bacteria with apical growth patterns, including the rod-shaped *C. glutamicum* and the filamentous *S. coelicolor* (7, 8). In the *scy* mutant, we detected a more intense and extended Van-FL signal in the tip-proximal part of the filaments (Fig. 3*B*), where a bulbous and bilobed Van-FL signal frequently marked apical branching or tip splitting. Moreover, the excess of Van-FL

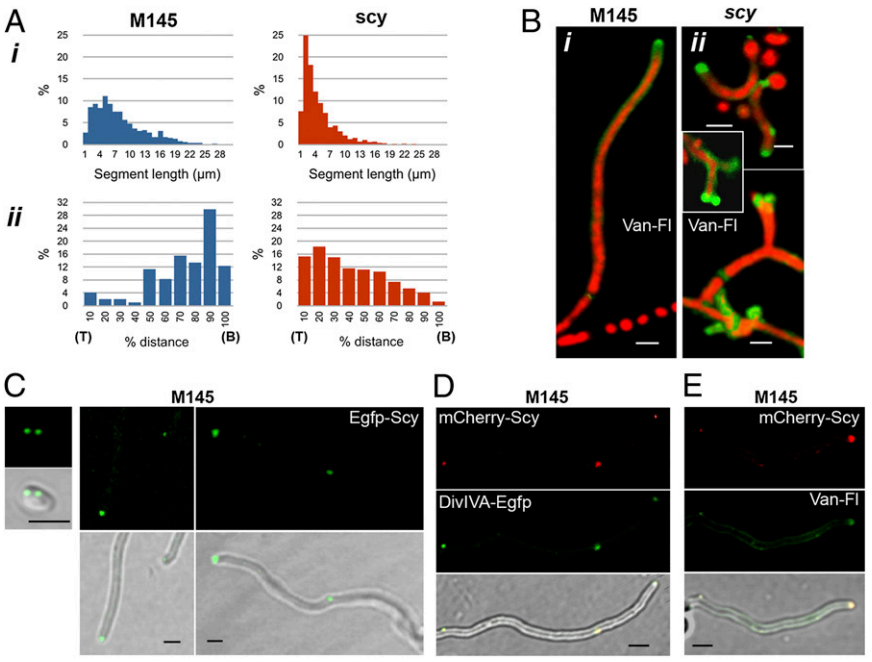

Fig. 3. Scy localizes to the tips and affects branching patterns and cell wall synthesis. (*A*) Statistical analysis of the segment length (*i*) and the relative location of new tip positions compared with the full-length of hyphal fragments already extending at their tip (*ii*). Around 300 branching hyphal networks, each originating from a single spore of either the WT or the *scy* mutant, were analyzed after 10–16 h of growth (Fig. S3). (*B*) Sites for new cell wall synthesis were monitored using Van-FL (green) and propidium iodide (red) staining of the WT (*i*) and *scy* mutant, K110 (*ii*), after 16 h of growth. (*C*) *S. coelicolor* M145/pK56, carrying *egfp-scy* under the control of the *scy* promoter, was grown for 16 h, and cells were viewed by laser-scanning confocal microscopy. The first image shows a spore before germination. Fluorescent images are positioned above the respective overlaid images with the bright-field views. (*D*) *S. coelicolor* M145/pKF59/pK57, carrying both *divIVA-egfp* (pKF59) and *mCherry-scy* (pK57), was cultivated for 16 h, and the cells were viewed as above. (*Upper*) Fluorescent images show the red and green channels for mCherry-Scy and DivIVA-Egfp, respectively. (*Lower*) Images show the overlaid view of both fluorescent channels, together with the bright-field views. (*E*) Van-FL staining of *S. coelicolor* M145/pK57 carrying *mCherry-Scy* grown for 16 h. (*Upper*) Fluorescent images show the red and green channels for mCherry-Scy and Van-FL, respectively. (*Lower*) Images show the overlaid view of both fluorescent channels, together with the bright-field view. (Scale bars: *B–E*, 1 μm.)

staining at lateral positions resulted in multiple branches originating from the same lateral sites.

Scy Localizes to Growing Tips and Marks the Sites for de Novo Tip Emergence. To establish the localization of Scy, we generated pK56, carrying an Egfp-Scy translational fusion under the control of the native *scy* promoter, allowing Egfp-Scy localization in the presence of native Scy. Apart from some hyphal meandering, pK56 fully complemented the branching defects and altered sporulation properties of K112, the unmarked null mutant of *scy,* confirming that Egfp-Scy was mostly functional. Egfp-Scy localized to growing established tips and young tips that had been formed recently. Bright Egfp-Scy foci were also identified in spores before germination at potential sites for germ tube outgrowth and at sites in the lateral hyphal wall, possibly marking the positions of future branch points (Fig. 3*C*). DivIVA, the known polarity determinant of *S. coelicolor*, was shown to localize to future tip positions ~30 min before the time when the dome of the tip became visible (14). Therefore, to confirm that Scy not only localized to existing tips but marked the positions of future tips, we localized Scy and DivIVA simultaneously using two different fluorescent fusions, mCherry-Scy and DivIVA-Egfp (Fig. 3*D*). The colocalization of mCherry-Scy and DivIVA-Egfp not only at the hyphal apex but at sites on the lateral wall confirmed that Scy, together with DivIVA, is implicated in the selection of sites for de novo tip formation.

Furthermore, to establish a link between Scy and cell wall synthesis, we monitored Van-FL incorporation, together with localization of mCherry-Scy (Fig. 3*E*). The colocalization of Van-FL and mCherry-Scy confirmed that, similar to DivIVA, Scy also marks the sites of new cell wall synthesis, which was not exclusive to growing tip ends but also to several distinct, lateral foci that presumably marked future branchpoints.

Multiple and Dispersed DivIVA Foci Promote Irregular Hyphal Extension in the *scy* Mutant. To test whether Scy controlled DivIVA localization, we compared DivIVA-Egfp localization in the WT

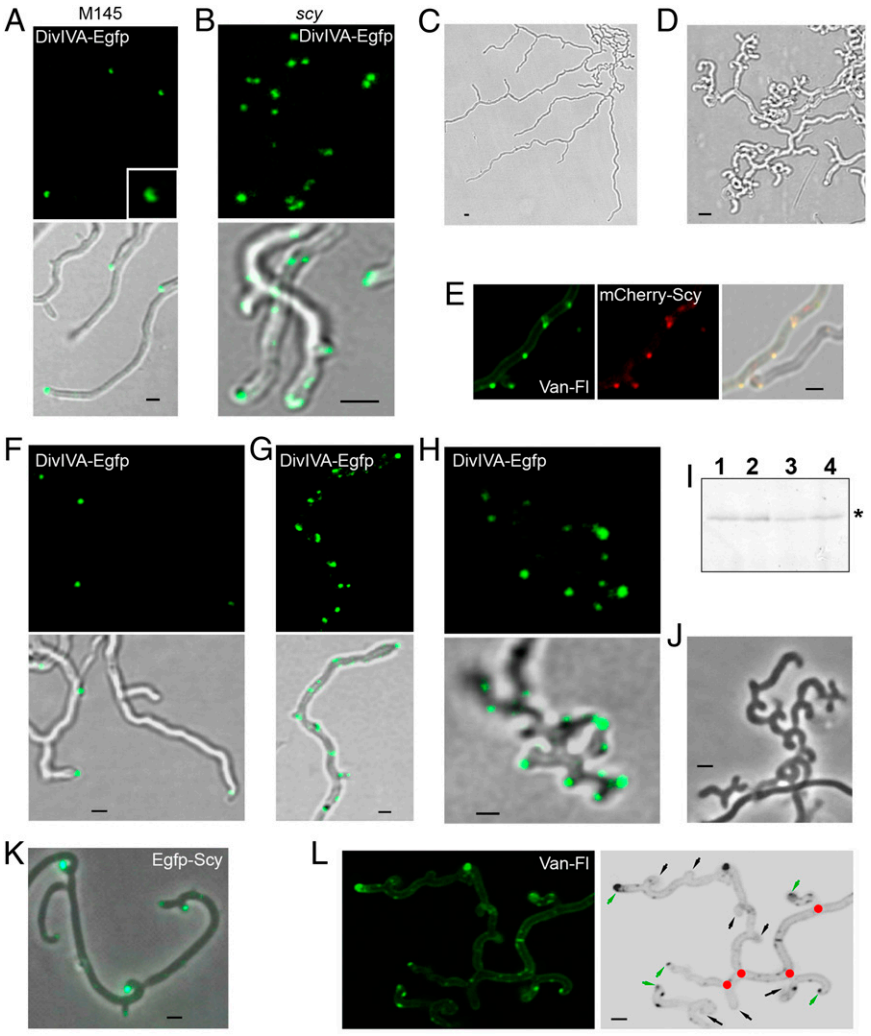

Fig. 4. Scy affects DivIVA localization and branching. DivIVA-Egfp was monitored in the WT (*A*) and in the *scy* mutant, K110 (*B*). *S. coelicolor* M145/pKF59 (*A*) and K110/pKF59 (*B*) were grown for 16 h. Both fluorescent (green) and overlaid images of green and bright-field views are shown. (*A*, *Inset*) Close-up of one of the dome-like DivIVA-Egfp localizations, consistent with DivIVA's apparent affinity for curved membranes (18, 19). (*C* and *D*) Effect of Scy overproduction on branching. *S. coelicolor* M145/pK48 carrying *scy* on a multicopy, autonomously replicating plasmid under the control of a thiostrepton-inducible promoter was cultivated for 16 h. Half of the culture was then induced with 20 μg/mL thiostrepton, whereas the other half continued growing in the absence of the inducer. After 3 h, hyphae of uninduced (*C*) and induced (*D*) samples were viewed using bright-field microscopy. (*E*) *S. coelicolor* M145/pK66/pK48 carrying *mCherry-scy* and a further copy of *scy* under the control of a thiostrepton-inducible promoter was grown for 16 h, when the samples were induced with 20 μg/mL thiostrepton. After 1 h, the cells were stained with Van-FL and viewed. The fluorescent images show the green (*Left*) and red (*Center*) channels for Van-FL and mCherry-Scy, respectively. (*Right*) Images show the overlaid view of both fluorescent channels, together with the bright-field view. (*F–H*) Effect of Scy overproduction on DivIVA localization. The plasmid pK48 carrying *scy* under the thiostrepton-inducible promoter was introduced into *S. coelicolor* M145/pKF59 carrying *divIVA-egfp*. *S. coelicolor* M145/pKF59/pK48 was grown for 16 h, when the cultures were induced with 20 μg/mL thiostrepton. Uninduced cells (*F*), together with thiostrepton-induced cells at 1 h (*G*) and 3 h (*H*) after induction, were viewed using laser-scanning confocal microscopy. Because of the irregular shape of the *scy* mutant (*B*) and the abundant branching after Scy overproduction (*H*), both samples generated 3D shapes. Therefore, instead of taking images from a single plane, we collected Z-stacks, and the averages generated by the internal TCS SP2 software are shown. (*I*) Cell extracts from samples generated as in *F–H* were analyzed using SDS/PAGE, and the fluorescence emission of DivIVA-Egfp was monitored using a phosphoimager (Molecular Imager FX; BioRad). Cells were collected at 1 h (lanes 1 and 2) and 3 h (lanes 3 and 4) after thiostrepton induction. Uninduced (lanes 1 and 3) and thiostrepton-induced (lanes 2 and 4) samples are shown. DivIVA-Egfp is marked with an asterisk. (*J*) Cultures generated as in *C* and *D* were induced with thiostrepton for 5 h, and the "hook-on-hook" growth pattern was viewed using phase-contrast microscopy. (*K*) *S. coelicolor* M145/pK52 carrying *egfp-scy* on a multicopy, autonomously replicating plasmid under the control of a thiostrepton-inducible promoter was cultivated for 16 h. The samples were then induced with 20 μg/mL thiostrepton for further 5 h and viewed using confocal microscopy. The bright-field and fluorescence images are overlaid. (*L*) (*Left*) Cells in *J* were stained with Van-FL to monitor new cell wall synthesis. (*Right*) Computer-generated, inverse, and grayscale image indicates the initial branchpoints during Scy induction (red circles), the actively growing tips (green arrows), and the tips with no apparent growth (black arrows). (Scale bars: *A–H* and *J–L*, 1 μm.)

and *scy* mutant. In WT hyphae, a single, point-like DivIVA-Egfp focus marked the new tip sites, followed by a more extended, dome-shaped DivIVA-Egfp signal that kept to the curvature of the tip (Fig. 4*A*). This is consistent with the recent demonstration that *B. subtilis* DivIVA binds to membranes with concave curvatures (18, 19). In contrast, in the *scy* mutant, the DivIVA foci appeared to be patchier and dispersed. At least ~76% of the DivIVA foci were within less than 1 μm from a neighboring DivIVA foci, and two to three DivIVA foci were found at ~40% of existing tips (Fig. 4*B*), consistent with apical branching in K110 (Figs. 2*C* and 3B). The multiple DivIVA patches, which promote cell wall extension at these irregular sites, can explain the asymmetrical tip curvature and uneven hyphal diameter of the *scy* mutant. This suggests that Scy controls the number and organization of the DivIVA complexes in the *Streptomyces* hyphae.

Overexpression of Scy Initiates Copious de Novo Tip Formation via Recruitment of DivIVA to Ectopic Locations. To understand how Scy controlled hyphal branching, we monitored the effect of Scy overproduction in *S. coelicolor* using pK48, a multicopy plasmid carrying *scy* under the control of a thiostrepton-inducible promoter. In the absence of thiostrepton, hyphal growth and branching of *S. coelicolor* M145/pK48 were indistinguishable from that of the WT, M145 (Fig. 4*C*). However, when Scy overproduction was induced in the presence of thiostrepton, there were dramatic effects on hyphal morphology, with the prolific emergence of new tips generating short and curved hyphae (Fig. 4*D*). To dissect the effect of Scy overproduction, we first monitored Scy itself by introducing the single-copy, integrative plasmid pK66 carrying *mCherry-scy*, together with the multicopy plasmid pK48 carrying the thiostrepton-inducible *scy*. After induction of Scy overproduction for 1 h, we observed the appearance of multiple mCherry-Scy foci, which localized to new cell wall synthesis when monitored using Van-FL staining (Fig. 4*E*). This suggested that Scy controlled the selection of sites for de novo tip production and the establishment of new cell wall synthesis during lateral branching.

The abundant emergence of new tips after the ectopic production of Scy was reminiscent of the effect of DivIVA overproduction (8, 14). To establish whether de novo tip formation in the Scy overproducing strain was via recruitment of DivIVA, we monitored DivIVA-Egfp after thiostrepton induction of Scy expression (Fig. 4 *F–H*). One hour after Scy induction, multiple DivIVA-Egfp foci were detected along the lateral hyphal wall, and these DivIVA-Egfp foci marked the location of new tips detected about 3 h after thiostrepton induction of Scy overproduction. This suggested that Scy can recruit DivIVA and mark the sites for de novo tip formation, generating lateral branching. Monitoring the level of DivIVA-Egfp using activity gels (Fig. 4*I*) confirmed that Scy overproduction had no effect on DivIVA levels, only on its localization. Interestingly, overproduction of Scy for a further 5 h produced a fractal-like, "hook-on-hook" growth pattern (Fig. 4*J*). Monitoring Egfp-Scy under these conditions confirmed the presence of Scy at the end of all of the "hooks" (Fig. 4*K*); however, Van-FL staining suggested abortive branching, because most of the hook ends lacked active cell wall synthesis apart from the last, leading hook (Fig. 4*L*). One possible explanation for this unusual growth pattern is that although Scy levels were high, levels of DivIVA, and presumably also levels of cell wall synthetic enzymes, were unchanged. Therefore, the repeated generation of a large number of actively growing tips could not be maintained, which led to abortive branching generating the hook-on-hook pattern.

Roles of Scy and DivIVA Are Closely Linked. Clearly, both the absence and overproduction of Scy had significant effects on DivIVA localization. Conversely, to test the effect of DivIVA on Scy localization, we monitored mCherry-Scy in the DivIVA-depleted strain, K115, and in the DivIVA overproducer, K114. The former strain has a chromosomal *divIVA* deletion but carries a single copy of *divIVA* under the thiostrepton-inducible promoter (8). In the presence of low levels of thiostrepton, K115 exhibits normal growth and branching and mCherry-Scy localizes at the growing tips (Fig. S4*A*). When K115 cells carrying mCherry-Scy were moved onto media lacking thiostrepton, although we observed the same hyphal deformations due to DivIVA depletion as described before (8), mCherry-Scy clearly localized to the hyphal tips (Fig. S4*B*). This might suggest that Scy does not require DivIVA for its polar localization. On the other hand, thiostrepton depletion does not completely abolish DivIVA synthesis in K115, and the low levels of DivIVA [1/10th of the WT levels (8)] might be sufficient for the recruitment of Scy. The DivIVA depletion studies suggest either that Scy can localize independent of DivIVA or that very little DivIVA is sufficient to recruit Scy.

When DivIVA was overproduced by exposing K114 carrying pK66 to high levels of thiostrepton, mCherry-Scy was detected at the multiple, ballooned tips (Fig. S4*D*), confirming that DivIVA can recruit Scy to newly established tip locations. To test whether overproduction of DivIVA affected Scy levels, we monitored mCherry-Scy in K114/pK66 after thiostrepton induction of DivIVA production (Fig. S4*E*); however, just as Scy overproduction did not change the DivIVA levels, DivIVA overproduction did not lead to elevated Scy levels.

Protein–Protein Interactions Confirm a Polar Assembly of Coiled-Coil Proteins. We tested whether colocalization of Scy and DivIVA was due to a direct interaction between these two proteins using a bacterial two-hybrid (BTH) assay, wherein two domains, T18 and T25, of a bacterial adenylate cyclase were fused to the N terminus of Scy or DivIVA. Protein–protein interactions were established when the appropriate T18 and T25 fusions restored a functional adenylate cyclase screened using a cAMP-dependent β-galactosidase assay. We have demonstrated interactions between T18-Scy and T25-Scy previously (22), suggesting either parallel homodimerization of Scy and/or interactions within a higher order assembly. All the homo- and hetero-pairs of T18-Scy, T25-Scy, T18-DivIVA, and T25-DivIVA were tested (Fig. 5*A*), and we could clearly demonstrate an in vivo interaction between Scy and DivIVA in the heterologous host *E. coli*.

To demonstrate direct interaction between Scy and DivIVA in vitro, both Scy and DivIVA were overexpressed, purified, and analyzed using a pelleting assay (Fig. 5*B*). After ultracentrifugation, the Scy, DivIVA, and Scy-DivIVA mixtures were analyzed using SDS/PAGE. The fact that Scy pulled DivIVA to the pellet fraction confirmed interactions between these two proteins. Moreover, Scy could form higher order assemblies with DivIVA even when the latter was present in excess (Fig. 5*C*). Although we do not know the stoichiometry of this interaction, the molar DivIVA/Scy ratio was higher than 3 in our in vitro assay. To assess the Scy-DivIVA interaction, we tested DivIVA, together with three different C-terminal Scy fragments, using the BTH assay (Fig. 5*D*). The positive interaction of DivIVA with all these Scy fragments suggests that Scy could function as a molecular scaffold and could sequester DivIVA, generating some form of higher order assembly.

The unusually long and regular C-terminal coiled-coil repeat could make Scy particularly suitable for the role of a molecular scaffold that can interact and organize numerous proteins at the hyphal tip. This raises the possibility of the existence of a multiprotein, polar assembly in *Streptomyces* similar to the polarisome found in yeast (23). To establish the presence of a multiprotein complex, we searched for other proteins that have already been localized to the tip in *S. coelicolor*. One of these, FilP, another coiled-coil protein that has noncanonical repeats (22), had been shown to form filaments within the *Streptomyces* hyphae with additional occasional tip localization (20). Interestingly, the gene

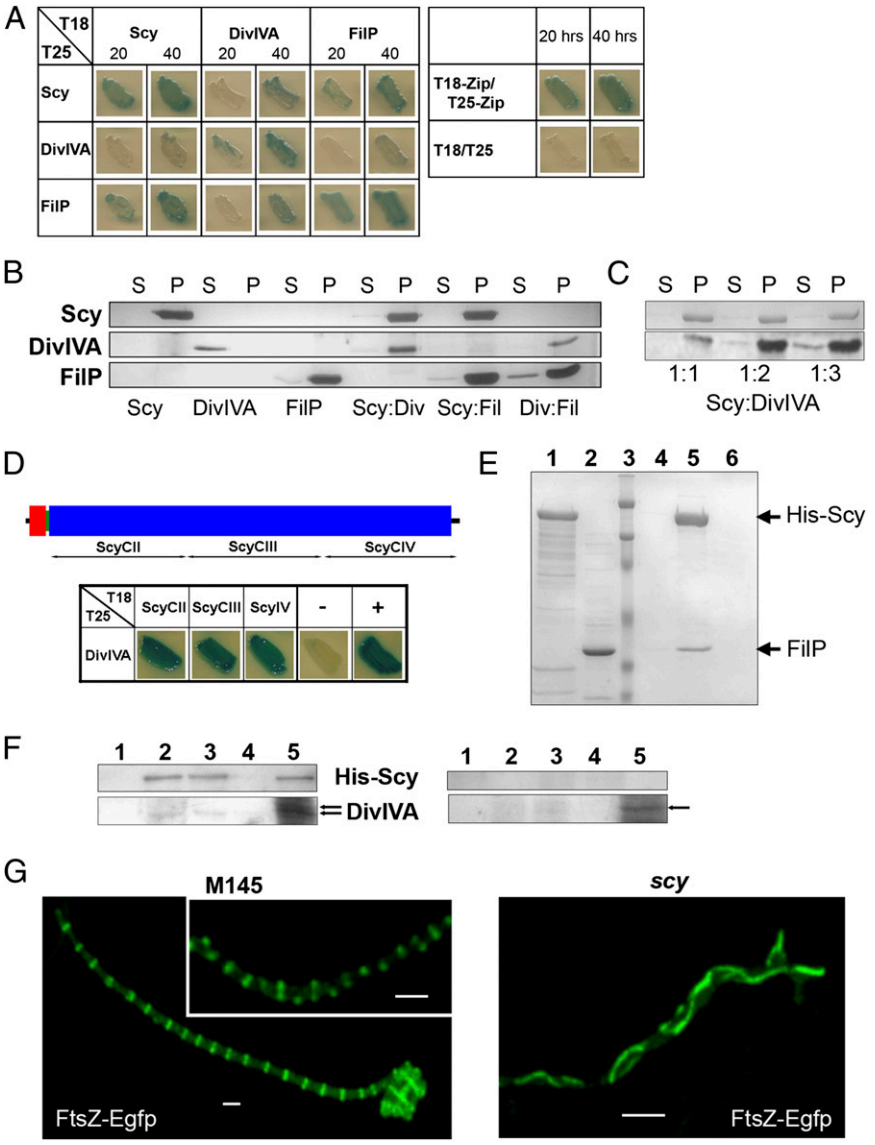

Fig. 5. Direct pairwise interactions between Scy, DivIVA, and FilP establish a multiprotein, polar assembly in *Streptomyces*. (*A* and *D*) Bacterial two-hybrid analysis. The appropriate pUT18c and pKT25 derivatives were introduced by cotransformation into BTH101, and the cotransformants were screened in LB containing 0.5 mM IPTG and 40 μg/mL Xgal after 20 h and 40 h (*A*) or 48 h (*D*) of incubation at 30 °C. The pUT18c and pKT25 vectors were used as a negative control, whereas the pUT18c-Zip and pKT25-Zip plasmid pair was used as a positive control (46). The N and C terminal domains of Scy (red and blue boxes, respectively) together with the Scy fragments tested are shown at the top of panel *D*. Blue streaks indicate protein–protein interactions by restoring adenylate cyclase activity, which, in turn, activates the β-galactosidase–dependent hydrolysis of Xgal. (*B* and *C*) Pelleting assay using ultracentrifugation. His-tagged Scy, DivIVA, and FilP and their pairwise mixtures were pelleted using ultracentrifugation. Both the pellet (P) and supernatant (S) fractions were analyzed using SDS/PAGE. (*E*) Affinity chromatography of His-Scy and FilP. His-Scy (lane 1) was immobilized onto a Ni-NTA spin-column. This was followed by the loading of cell extracts of BL21(DE3)pLysS/pK71 containing overexpressed FilP (lane 2). After washes (lane 3, last wash), the column-bound proteins were eluted by raising the imidazole concentration to 500 mM (lane 5). An elution sample was also generated by repeating the experiment without loading His-Scy onto the column (lane 6). A molecular mass marker indicates 200, 116, 66, 45, and 31 kDa (lane 3). (*F*) *S. coelicolor* M145/pK48 expressing His-Scy under the control of a thiostrepton-inducible promoter was cultivated for 12 h. Half of the cells were then induced with 1 μg/mL thiostrepton, whereas the other half continued growing in the absence of the inducer. After further growth for 7 h, cell lysates (lane 5) of uninduced (*Right*) and induced (*Left*) samples were applied onto a Ni-NTA spin-column. After washes (lane 1, last wash), the samples (lanes 2–4) were eluted by raising the imidazole concentration to 500 mM and were analyzed using an anti-DivIVA antibody (45). Arrows mark DivIVA identified by the antibody. (*G*) Deletion of *scy* affects cell division. Localization of FtsZ-Egfp was monitored in the aerial hyphae of the WT strain, *S. coelicolor* M145/pKF41 (*Left*) and the *scy* mutant, K112/pKF41 (*Right*) are shown. All strains were grown for 44 h alongside microscope coverslips to allow viewing of aerial development and sporulation. (Scale bars: 1 μm.)

(*SCO5396*) encoding FilP lies immediately downstream of *scy* in the chromosome, and the weaker cell wall of the *filP* mutant, as revealed by atomic force microscopy, suggested some role in the control of cell shape (20).

To establish whether FilP was part of a polar assembly, we tested any potential interactions between FilP and Scy or DivIVA both in vivo using BTH assays (Fig. 5*A*) and in vitro by pelleting using ultracentrifugation (Fig. 5*B*). In the BTH assays, FilP showed strong interaction with Scy and a weaker interaction with DivIVA. In the pelleting assay, FilP pulled DivIVA to the pellet fraction, confirming their interaction in vitro. Because both Scy and FilP were in the pellet fractions after ultracentrifugation, to demonstrate Scy–FilP interactions in vitro, we performed an affinity coelution test. According to this, His-Scy, when immobilized onto a nickel-nitriloacetic acid (Ni-NTA) column, was able to retain nontagged FilP from cell extracts, whereas FilP on its own did not bind to the Ni-NTA column, confirming interactions between Scy and FilP (Fig. 5*E*).

To show that Scy and DivIVA were part of the same assembly within *Streptomyces*, we demonstrated that His-tagged Scy, which was expressed in *Streptomyces*, copurified with DivIVA when Ni-affinity chromatography was used (Fig. 5*F*). Although the amount of DivIVA coeluted with His-Scy was low, it was significantly higher compared with that in the control cell extracts, where very little, if any, His-Scy was present. Interestingly, in one of the preload samples, we detected multiple bands of DivIVA presumably corresponding to its different phosphorylated forms (24). The single DivIVA band that coeluted with His-Scy could indicate that Scy might interact only with a specific form of DivIVA.

Lack of Scy also Affects Cell Division. During vegetative growth and in the initial phase of aerial growth, *S. coelicolor* forms long, multigenomic filaments, thereby not fully completing cell division at these stages of the life cycle. Chromosome segregation and cell-cell separation are only accomplished during sporulation, where 50–100 unigenomic prespore compartments are created synchronously within a single sporogenic aerial hypha following the ladder-like positioning of FtsZ and chromosome segregation aided by the ParA/ParB complex (2). Unlike in most unigenomic bacteria, where incomplete cell division is lethal, null mutations of cell division genes, such as *ftsZ* or *ftsK*, affect only sporulation but not hyphal growth in *S. coelicolor*. The *scy*

mutant produced significantly fewer spores (10%) than the WT, and the irregularly spaced and often tilted sporulation septation and the uneven chromosome distribution in the spore chains suggested that cell shape and cell division were both affected in cells lacking Scy (Fig. 2 and Fig. S2). To test the effect of Scy on cell division, we monitored FtsZ localization in both WT and *scy* mutant strains by introducing pKF41 (25) carrying *ftsZ-egfp*. In the WT strain, FtsZ-Egfp rings were easily detectable and were positioned as in a ladder, marking the sites for future sporulation septation (Fig. 5*G*). However, in K112/pKF41, there were very few aerial hyphae, with short, unsynchronized stretches of noticeable but very faint FtsZ-Egfp rings. Instead, strong FtsZ-Egfp cables were detected in the majority (~80%) of the aerial hyphae of K112/pKF41, which did not show sporulation septation and where, instead of discrete and orderly FtsZ rings, long, loosely curved FtsZ cables run alongside and often parallel to the lateral walls of the hyphae (Fig. 5*G*).

Discussion

Scy Is a Long Coiled-Coil Protein with Multiple Partners. Scy is unusually long, and it is dominated by a novel repeat that appears to form a continuous coiled coil, constituting >90% of the whole sequence. If indeed this is an uninterrupted single domain, its length exceeds those of any previously characterized bacterial or archaeal coiled-coil domain (26), although it is slightly shorter than two eukaryotic proteins, the spindle pole component NuMA (1,500 amino acids) and the Golgi-localized Giantin (3,150 amino acids). The most notable feature of Scy is the nature of the coiled-coil repeat in this long domain, which is compatible with a 51-mer repeat that can be interpreted as a hendecad (11-mer) repeat modified by an extra seven residues after every four repeats. Although there are cases of highly periodically modified heptad repeats (27), we are unaware of such a regular modification of hendecad repeats in any other protein.

Although no structural studies are available, Scy was suggested to form parallel homodimer coiled coils (22). These homodimers are likely to form higher order assemblies, because soluble Scy preparations pelleted when exposed to ultracentrifugation (Fig. 5*B*). We have shown that Scy directly interacted with the filament-forming protein FilP and the polarity marker DivIVA in vitro, and we have shown that Scy and DivIVA colocalized in vivo at newly established and growing tips. Both the BTH assay (Fig. 5*D*) and the pelleting assay (Fig. 5*C*) confirmed that Scy can bind multiple DivIVAs throughout its long C-terminal domain. This suggests that Scy can accommodate, sequester, and organize several of its partner proteins.

Tip Organizing Center for Selecting, Establishing, and Maintaining Polarized Growth in Filamentous Bacteria. In eukaryotes, polarized growth requires landmark proteins to select specific sites and a complex assembly that recruits vesicles for cell membrane or cell wall expansion (1). In budding yeast, the complex assembly of proteins, called the "polarisome," is essential for the organization of the actin cytoskeleton, which forms cables for vesicle transport to the bud site. In filamentous fungi, the Spitzenkörper or apical body functions as the vesicle supply center at the growing hyphal tip. Here, we provide evidence that multiprotein assemblies for organizing polarized growth are not restricted to eukaryotes, because tip extension of the filamentous bacterium *S. coelicolor* is also controlled by a complex assembly of proteins, namely, the tip organizing center (TIPOC). The first identifed components of the TIPOC include the molecular organizer Scy and the positional marker DivIVA (Fig. 6). Scy, together with DivIVA, localized to established hyphal tips and also to lateral sites marking the positions of future branches and new cell wall synthesis. The contribution of FilP to the functional TIPOC remains to be analyzed in detail. Clearly, FilP can interact with both Scy and DivIVA at the tip, but it also forms strong filaments along the hyphae, a pattern so far specific to FilP (20). It is particularly interesting that all three proteins, Scy, DivIVA, and FilP, are coiled-coil proteins with highly similar domain organization: a short coiled-coil domain, followed by a linker and a second coiled-coil domain (22). In addition to other bacterial examples of coiled-coil polarity determinants, such as TipN or PopZ of *C. crescentus* (28–32), the spindle pole body, specialized for centromere function in yeast, is also dominated by long coiled-coil proteins (33, 34), suggesting further structural similarities between organizing centers in bacteria and eukaryotes.

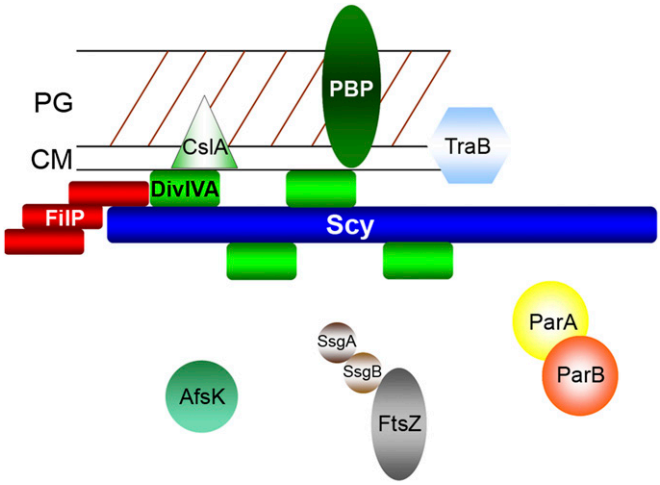

Fig. 6. TIPOC serves as a "hub" for polarized growth. The long, coiled-coil protein Scy directly interacts with DivIVA and FilP at hyphal tips. DivIVA directly controls cell wall synthesis (PBP), whereas Scy is responsible for the organization of the TIPOC. The possible link between the cell division machinery (FtsZ, SsgA, SsgB, ParA, and ParB) and the TIPOC is also shown. Other tip-localized proteins include CslA (cellulose synthase), TraB (DNA translocase) and AfsK, the kinase that can phosphorylate DivIVA. CM, cell membrane; PG, peptidoglycan.

We believe that the evidence for a TIPOC is strong, and further components of the polar assembly are expected to emerge. It will be of interest to establish whether any of the previously tip-localized proteins, such as TraB, a DNA-translocating ATPase that is essential for conjugal plasmid transfer (35), or CslA, a cellulose synthase that is suggested for the production of the extracellular polysaccharide matrix and was shown to interact with DivIVA (36) (Fig. 6), are indeed organized by the TIPOC.

Link Between Polarized Growth and Cell Division? The *scy* mutant showed severe defects in cell division during sporulation, producing spore compartments with different amounts of DNA (Fig. 2 *D*–*G*). Segregation of chromosomes is controlled by ParA and ParB in *S. coelicolor* and, interestingly, ParA forms distinct foci at the tips of the aerial hyphae before polymerization into ParA helices that act as scaffolds for the regular arrangement of ParB foci along the sporogenic aerial hyphae (37). It is conceivable that the nucleation of ParA at the tip of the aerial hyphae depends on the TIPOC. Indeed, interaction between *Streptomyces* DivIVA and ParB has been demonstrated, albeit in the heterologous host *E. coli* (38). We have also shown that localization of FtsZ was compromised in the *scy* mutant (Fig. 5*G*). Instead of FtsZ ladders that precede septation in WT *S. coelicolor*, long FtsZ filaments often run parallel to the axis of the sporogenic aerial hyphae. FtsZ positioning at midcell of the rod-shaped *E. coli* or *B. subtilis* relies on two mechanisms: nucleoid occlusion and polar sequestration of the division inhibitors, MinD and MinC (17). In *S. coelicolor*, sporulation septa formation precedes chromosome segregation (2); thus, the nucleoid occlusion mechanism is unlikely. Moreover, *S. coelicolor* has no obvi-

ous MinC or MinE homologs. Recently, FtsZ positioning in *S. coelicolor* was shown to be under positive control by an FtsZ partner protein, SsgB, which, in turn, depends on SsgA (39). Interestingly, SsgA localizes at the hyphal tips in a dynamic fashion (40); therefore, it could, in principle, be part of the TIPOC (Fig. 6). Although it is very attractive to propose a direct link between the TIPOC and cytokinesis, we cannot rule out an indirect link because the severe defect of the hyphal geometry of the *scy* mutant might affect spatial cues for the formation of the FtsZ ladder.

Scy Is Important for the Assembly and Integrity of the TIPOC. Although the roles of DivIVA and Scy are very closely linked, we can distinguish their individual contribution to establishing polarity in *Streptomyces*. DivIVA is essential for branching and polarized growth, and it directly recruits the cell wall synthetic machinery. For the latter, we have only indirect, although strong, evidence. First, direct interaction between DivIVA and PBP3 was shown in another actinomycete, *M. tuberculosis* (16). Furthermore, during DivIVA overproduction, isotropic tip expansion was observed (8) (Fig. S4*D*), which was inhibited by bacitracin, a cell wall synthesis inhibitor, demonstrating that the ballooning tip expansion was dependent on active cell wall synthesis (14). Scy overproduction did not lead to similar ballooning tips but, instead, generated copious branching followed by a hook-on-hook hyphal growth pattern in which only selected tips were actively growing (Fig. 4). This suggested that although Scy controlled the number of tips established, it did not directly recruit the cell wall synthetic enzymes. Also, deletion of *scy* did not abolish tip formation. On the contrary, it promoted overbranching; thus, Scy is not essential for tip formation, per se.

Identifying the mechanism for DivIVA positioning and organization is the key to establishing a new polarity center in *Streptomyces*. Special compositional cues of the membrane might act as site-specific markers. Anionic phospholipids localized to tips and branchpoints in *S. coelicolor*, and changing the levels of these phospholipids altered branching and hyphal geometry (41). In *B. subtilis*, membrane composition was suggested to affect the localization of transmembrane proteins that stabilize the MreB cables (15). More importantly, a geometrical cue, negative membrane curvature, was shown to recruit DivIVA to the poles and division sites in the rod-shaped *B. subtilis* (18, 19). However, unlike the limited sites of convex membrane curvatures in *B. subtilis*, the long and often meandering *Streptomyces* hyphae have numerous convex curvatures that could, in principle, target DivIVA to these sites. Although most of the new branch points appear to be from convex hyphal curvatures (14), there are many more negative hyphal curvatures than emerging tips; thus, although membrane curvature might facilitate DivIVA recruitment, *Streptomyces* must have a mechanism to restrict DivIVA to selected sites only. We propose that it is the Scy assembly, which, by sequestering multiple DivIVA tetramers (42), regulates the number of DivIVA foci, and therefore controls the number of polarity centers in *Streptomyces*.

Lack of Scy produces multiple polarity centers, suggesting that Scy assemblies can limit the number of TIPOCs established, perhaps by organizing the otherwise more dispersed DivIVA assemblies into a limited number of polarity centers. Overproduction of both Scy and DivIVA also results in an increasing number of new polarity centers, confirming that the cellular levels of the TIPOC components can control the assembly of the TIPOC and de novo tip emergence. On the other hand, the dispersal of the DivIVA patches at existing tips of the *scy* mutant suggests that Scy is important not only for the assembly of the TIPOC but for the integrity of existing, actively growing tips. Hence, lack of Scy will destabilize the TIPOC, leading to the dispersal of DivIVA patches followed by the emergence of new tips. Recently, it was shown that new branches can be initiated by DivIVA complexes breaking off from existing tips and initiating new tip emergence. Mathematical modeling supported the mechanism whereby increasing DivIVA levels at already established and growing tips result in tip focus splitting (43). Similarly, when Scy is overproduced in the presence of unchanging DivIVA levels, the hook-on-hook growth pattern is compatible with the dispersal of excess TIPOC components, in this case Scy, generating Scy-containing but not actively growing hook tips, together with Scy-DivIVA assemblies at the growing tip (Fig. 4 *J–L*). Interestingly, DivIVA phosphorylation at the hyphal tip by AfsK, a Ser/Thr kinase, was shown to affect branching in *Streptomyces* (24). Therefore, it will be of special interest to establish in the future how AfsK is recruited to the tips and what the effect of DivIVA phosphorylation is on Scy-DivIVA interaction and the integrity of the TIPOC.

The suggested mechanism for controlling the assembly and integrity of a bacterial polarity center by the sequestration and organization of a multiprotein polarity complex, the TIPOC, is consistent with our experimental findings, and it reconciles the apparent paradox concerning the nucleation of multiple polarity centers both in the absence and excess of a polarity determinant. We propose that the TIPOC, including Scy, serves not only as a "hub" for polarized growth but, indirectly or directly, for coordinating cell division during sporulation in *Streptomyces*.

Materials and Methods

Bacterial Strains and Growth Conditions. All bacterial strains, plasmids, and oligonucleotides used in this work are listed in Tables S1–S3, respectively. Generation of KO mutants and all plasmid constructions is detailed in *SI Materials and Methods*. Plasmids were introduced into *S. coelicolor* using conjugation via *E. coli* ET12567/pUZ8002, with the exception of pKF59, which was introduced into *S. coelicolor* using protoplast transformation (44). *Streptomyces* strains were grown at 30 °C on soya flour medium (SFM) containing 1% mannitol (44).

Overexpression and Purification of Scy, DivIVA, and FilP. Plasmid pGS2 was introduced to *E. coli* BL21 (DE3)pLysS (Novagen). Cultures of BL21(DE3)pLysS/pGS2 were grown at 37 °C for 3 h and, after induction with 1 mM isopropyl-β-D-thiogalactopyranoside (IPTG), for a further 4 h. After harvesting the mycelium, His-Scy was purified from the supernatant of cell lysates in buffer A: 50 mM NaH_2PO_4, 500 mM NaCl, and 10 mM imidazole under native conditions using a HisTrap HP 1-mL affinity column (GE Healthcare). After washing with buffer A containing 30 mM imidazole, His-Scy was eluted with a linear gradient of 30–300 mM imidazole in buffer A. His-Scy fractions were dialyzed against 20 mM Tris·HCl (pH 8) and further purified using a MonoQ 5/50 anion exchange column (GE Healthcare). Elution was carried out using a linear gradient of 0.01–1 M NaCl in 20 mM Tris·HCl (pH 8.0). Fractions containing His-Scy were dialyzed against 10 mM NaH_2PO_4 (pH 8.0) and were used for CD spectroscopy.

For the ultracentrifugation and affinity coelution studies, His-Scy, His-DivIVA, and His-FilP were purified with a simplified version of the above. Accordingly, cultures of BL21(DE3)pLysS carrying pGS2, pK68, and pK70 were grown at 37 °C for 3 h and, after induction with 1 mM IPTG, for a further 4 h. The His-tagged proteins were eluted with a step elution of 300 mM imidazole in buffer A, and the fractions were dialyzed either against 20 mM Tris·HCl and 200 mM NaCl (pH 8) for the ultracentrifugation or against 50 mM NaH_2PO_4, 300 mM NaCl, and 10 mM imidazole for the affinity coelution studies.

For the ultracentrifugation assays, the purified proteins were measured using a Bradford assay (Bio-Rad), and ~1-μM proteins were incubated at 30 °C for 20 min and spun at 100,000 × *g* for 30 min at 4 °C. The supernatant and the pellet were analyzed on 10% (wt/vol) PAGE.

Affinity Coelution of FilP with His-Scy. Purified His-Scy was immobilized onto a Ni-NTA spin-column (Qiagen) and was exposed to cell extracts from BL21 (DE3)pLysS/pK71 containing overexpressed FilP (nontagged) in a buffer (50 mM NaH_2PO_4, 300 mM NaCl, 20 mM $MgCl_2$, and 50 mM imidazole) optimized to avoid binding of nontagged proteins to the column. After several washes, His-Scy was eluted using 500 mM imidazole and the eluted samples were analyzed on 10% (wt/vol) PAGE. As a control, the experiment was repeated without loading His-Scy onto the Ni-NTA column to confirm that FilP on its own did not bind to the column.

Affinity Coelution of DivIVA with His-Scy from *Streptomyces*. *S. coelicolor* M145/pK48 expressing His-Scy under the control of a thiostrepton-inducible

promoter was cultivated for 12 h. Half of the samples were then induced using a low level of 1 μg/mL thiostrepton, whereas the other half continued growing in the absence of the inducer. After further growth for 7 h, cell lysates of uninduced and induced samples were applied onto a Ni-NTA spin-column in a buffer of 50 mM NaH_2PO_4 and 300 mM NaCl. After several washes, His-Scy was eluted by raising the imidazole concentration to 500 mM and the samples were analyzed on 8% (wt/vol) PAGE. Western blot analysis utilizing anti-DivIVA primary antibody (45) raised in rabbit diluted at 1:10,000 and a secondary antibody of anti-rabbit IgG-HRP conjugate (DAKO) diluted at 1:5,000 was used to confirm that DivIVA copurified with His-Scy from *Streptomyces* cell extracts.

Microscopy. ***Light microscopy.*** For laser-scanning confocal microscopy and for statistical analysis, spores were inoculated on the surface of cellophane membranes positioned on solid SFM medium to restrict hyphal growth in two dimensions when hyphal characteristics were monitored. When the purpose of the study was aerial development and sporulation, spores were inoculated alongside microscope coverslips inserted at angles of 45° into SFM medium. Cells on both cellophane membrane and coverslips were fixed with ice-cold methanol for 1 min before further staining with WGA-Alexa488 (50 μg/mL; Molecular Probes) and/or propidium iodide (25 μg/mL; Sigma) for 20 min. After several washes with water, samples were mounted using 20% (vol/vol) glycerol and viewed using a Leica TCS SP2 laser-scanning confocal microscope with a 63×, 1.4-N.A. oil immersion objective. Staining of nascent peptidoglycan was performed by staining the growing cells with 1 μg/mL BODIPY Van FL (Molecular Probes) and 1 μg/mL unlabeled vancomycin (Sigma) for 5 min.

TEM. Colonies were fixed with 2% (vol/vol) glutaraldehyde in 0.05 M sodium cacodylate (pH 7.0), stained with osmic acid, and embedded in LR White resin (The London Resin Co.) according to the manufacturer's instructions. After sectioning, the samples were examined in a Jeol 1200 EX transmission electron microscope at 80 KV and tagged image file format (TIFF) files were generated using a Deben AMT 1.3k camera.

Protein samples of His-Scy in 20 mM Tris and 150 mM NaCl (pH 8.0) were negatively stained using freshly prepared 2% ammonium molybdate (pH 8.0) on a 400-mesh copper grid with a carbon-coated pyroxylin support film. The grids were viewed at 200 kV in a Tecnai 20 transmission electron microscope (FEI) fitted with an AMT XR60B digital camera (Deben), and digital TIFF images were saved.

ACKNOWLEDGMENTS. We thank Kim C. Findlay and Richard Ewans-Gowing for assistance with the TEM and SEM; George Smith, Laura Kerry, and James Hunter for generating some of the constructs; and Ruchita Desai for technical assistance. We also thank Bartek Ditkowski and Dagmara Jakimowicz for sharing some of their constructs prior to publication and Prof. Richard Morris for stimulating discussions. We are very grateful to Prof. Sir David Hopwood, Prof. Andy Johnston, and Dr. Margaret Wexler for their valuable comments on the manuscript. This work was supported by Royal Society Research Grant 23646 (to G.H.K.), the John and Pamela Salters Foundation (G.H.K.), and Biotechnology and Biological Sciences Research Council Studentship BB/D526196/1 (to N.A.H.).

1. Nelson WJ (2003) Adaptation of core mechanisms to generate cell polarity. *Nature* 422(6933):766–774.
2. Flärdh K, Buttner MJ (2009) *Streptomyces* morphogenetics: Dissecting differentiation in a filamentous bacterium. *Nat Rev Microbiol* 7(1):36–49.
3. Cabeen MT, Jacobs-Wagner C (2010) The bacterial cytoskeleton. *Annu Rev Genet* 44: 365–392.
4. Pinho MG, Errington J (2003) Dispersed mode of *Staphylococcus aureus* cell wall synthesis in the absence of the division machinery. *Mol Microbiol* 50(3):871–881.
5. Ausmees N, Kuhn JR, Jacobs-Wagner C (2003) The bacterial cytoskeleton: An intermediate filament-like function in cell shape. *Cell* 115(6):705–713.
6. Charbon G, Cabeen MT, Jacobs-Wagner C (2009) Bacterial intermediate filaments: In vivo assembly, organization, and dynamics of crescentin. *Genes Dev* 23(9):1131–1144.
7. Daniel RA, Errington J (2003) Control of cell morphogenesis in bacteria: Two distinct ways to make a rod-shaped cell. *Cell* 113(6):767–776.
8. Flärdh K (2003) Essential role of DivIVA in polar growth and morphogenesis in *Streptomyces coelicolor* A3(2). *Mol Microbiol* 49(6):1523–1536.
9. Mazza P, et al. (2006) MreB of *Streptomyces coelicolor* is not essential for vegetative growth but is required for the integrity of aerial hyphae and spores. *Mol Microbiol* 60(4):838–852.
10. Heichlinger A, et al. (2011) The MreB-like protein Mbl of *Streptomyces coelicolor* A3 (2) depends on MreB for proper localization and contributes to spore wall synthesis. *J Bacteriol* 193(7):1533–1542.
11. Kleinschnitz EM, et al. (2011) Proteins encoded by the *mre* gene cluster in *Streptomyces coelicolor* A3(2) cooperate in spore wall synthesis. *Mol Microbiol* 79(5): 1367–1379.
12. McCormick JR, Su EP, Driks A, Losick R (1994) Growth and viability of *Streptomyces coelicolor* mutant for the cell division gene *ftsZ*. *Mol Microbiol* 14(2):243–254.
13. Flärdh K (2010) Cell polarity and the control of apical growth in *Streptomyces*. *Curr Opin Microbiol* 13(6):758–765.
14. Hempel AM, Wang SB, Letek M, Gil JA, Flärdh K (2008) Assemblies of DivIVA mark sites for hyphal branching and can establish new zones of cell wall growth in *Streptomyces coelicolor*. *J Bacteriol* 190(22):7579–7583.
15. Margolin W (2009) Sculpting the bacterial cell. *Curr Biol* 19(17):812–822.
16. Mukherjee P, et al. (2009) Novel role of Wag31 in protection of mycobacteria under oxidative stress. *Mol Microbiol* 73(1):103–119.
17. Wu LJ, Errington J (2012) Nucleoid occlusion and bacterial cell division. *Nat Rev Microbiol* 10(1):8–12.
18. Ramamurthi KS, Losick R (2009) Negative membrane curvature as a cue for subcellular localization of a bacterial protein. *Proc Natl Acad Sci USA* 106(32):13541–13545.
19. Lenarcic R, et al. (2009) Localisation of DivIVA by targeting to negatively curved membranes. *EMBO J* 28(15):2272–2282.
20. Bagchi S, Tomenius H, Belova LM, Ausmees N (2008) Intermediate filament-like proteins in bacteria and a cytoskeletal function in *Streptomyces*. *Mol Microbiol* 70(4):1037–1050.
21. Lupas A, Van Dyke M, Stock J (1991) Predicting coiled coils from protein sequences. *Science* 252(5009):1162–1164.
22. Walshaw J, Gillespie MD, Kelemen GH (2010) A novel coiled-coil repeat variant in a class of bacterial cytoskeletal proteins. *J Struct Biol* 170(2):202–215.
23. Moseley JB, Goode BL (2006) The yeast actin cytoskeleton: From cellular function to biochemical mechanism. *Microbiol Mol Biol Rev* 70(3):605–645.
24. Hempel AM, et al. (2012) The Ser/Thr protein kinase AfsK regulates polar growth and hyphal branching in the filamentous bacteria *Streptomyces*. *Proc Natl Acad Sci USA* 109(35):2371–2379.
25. Grantcharova N, Lustig U, Flärdh K (2005) Dynamics of FtsZ assembly during sporulation in *Streptomyces coelicolor* A3(2). *J Bacteriol* 187(9):3227–3237.
26. Rose A, Schraegle SJ, Stahlberg EA, Meier I (2005) Coiled-coil protein composition of 22 proteomes—Differences and common themes in subcellular infrastructure and traffic control. *BMC Evol Biol* 5:66.
27. Lupas AN, Gruber M (2005) The structure of alpha-helical coiled coils. *Adv Protein Chem* 70:37–78.
28. Huitema E, Pritchard S, Matteson D, Radhakrishnan SK, Viollier PH (2006) Bacterial birth scar proteins mark future flagellum assembly site. *Cell* 124(5):1025–1037.
29. Lam H, Schofield WB, Jacobs-Wagner C (2006) A landmark protein essential for establishing and perpetuating the polarity of a bacterial cell. *Cell* 124(5):1011–1023.
30. Bowman GR, et al. (2008) A polymeric protein anchors the chromosomal origin/ParB complex at a bacterial cell pole. *Cell* 134(6):945–955.
31. Ebersbach G, Briegel A, Jensen GJ, Jacobs-Wagner C (2008) A self-associating protein critical for chromosome attachment, division, and polar organization in *Caulobacter*. *Cell* 134(6):956–968.
32. Bowman GR, et al. (2010) *Caulobacter* PopZ forms a polar subdomain dictating sequential changes in pole composition and function. *Mol Microbiol* 76(1):173–189.
33. Zizlsperger N, Malashkevich VN, Pillay S, Keating AE (2008) Analysis of coiled-coil interactions between core proteins of the spindle pole body. *Biochemistry* 47(45): 11858–11868.
34. Zizlsperger N, Keating AE (2010) Specific coiled-coil interactions contribute to a global model of the structure of the spindle pole body. *J Struct Biol* 170(2):246–256.
35. Reuther J, Gekeler C, Tiffert Y, Wohlleben W, Muth G (2006) Unique conjugation mechanism in mycelial streptomycetes: A DNA-binding ATPase translocates unprocessed plasmid DNA at the hyphal tip. *Mol Microbiol* 61(2):436–446.
36. Xu H, Chater KF, Deng Z, Tao M (2008) A cellulose synthase-like protein involved in hyphal tip growth and morphological differentiation in *Streptomyces*. *J Bacteriol* 190(14):4971–4978.
37. Jakimowicz D, Zydek P, Kois A, Zakrzewska-Czerwińska J, Chater KF (2007) Alignment of multiple chromosomes along helical ParA scaffolding in sporulating *Streptomyces* hyphae. *Mol Microbiol* 65(3):625–641.
38. Donovan C, Sieger B, Krämer R, Bramkamp M (2012) A synthetic *Escherichia coli* system identifies a conserved origin tethering factor in Actinobacteria. *Mol Microbiol* 84(1):105–116.
39. Willemse J, Borst JW, de Waal E, Bisseling T, van Wezel GP (2011) Positive control of cell division: FtsZ is recruited by SsgB during sporulation of *Streptomyces*. *Genes Dev* 25(1):89–99.
40. Noens EE, et al. (2007) Loss of the controlled localization of growth stage-specific cell-wall synthesis pleiotropically affects developmental gene expression in an *ssgA* mutant of *Streptomyces coelicolor*. *Mol Microbiol* 64(5):1244–1259.
41. Jyothikumar V, et al. (2012) Cardiolipin synthase is required for *Streptomyces coelicolor* morphogenesis. *Mol Microbiol* 84(1):181–197.
42. Oliva MA, et al. (2010) Features critical for membrane binding revealed by DivIVA crystal structure. *EMBO J* 29(12):1988–2001.
43. Richards DM, Hempel AM, Flärdh K, Buttner MJ, Howard M (2012) Mechanistic basis of branch-site selection in filamentous bacteria. *PLOS Comput Biol* 8(3):e1002423.
44. Kieser T, Bibb MJ, Buttner MJ, Chater KF, Hopwood DA (2000) *Practical Streptomyces Genetics* (The John Innes Foundation, Norwich, UK).
45. Wang SB, et al. (2009) Domains involved in the in vivo function and oligomerization of apical growth determinant DivIVA in *Streptomyces coelicolor*. *FEMS Microbiol Lett* 297(1):101–109.
46. Karimova G, Pidoux J, Ullmann A, Ladant D (1998) A bacterial two-hybrid system based on a reconstituted signal transduction pathway. *Proc Natl Acad Sci USA* 95(10): 5752–5756.